

HIGH FIDELITY EDGE AWARE NORMAL ESTIMATION FOR LOW RESOLUTION AND NOISY POINT CLOUDS OF HERITAGE SITES

Joelle Abu-Hani*, Tian Zhang, Sagi Filin

Mapping and Geo-Information Engineering, Technion – Israel Institute of Technology, Haifa, Israel
(abu.h, tianz, filin)@technion.ac.il

Commission II, WG 8

KEY WORDS: Point clouds, L_0 optimization, Robust Normal Estimation, Cultural Heritage

ABSTRACT:

Surface normals play a pivotal role in most shape analysis applications. As such, their accurate computation has received a considerable amount of attention over the years. In heritage sites, where entities of complex shape are prevalent, the development of reliable means to estimate them becomes even more important. When approaching the computation of normals, not only the shape complexity becomes a factor, but also the nature of the data, specifically the point density and noise level. To handle both shape and data quality-related aspects, this paper proposes a new method for the computation of surface normals, focusing on entities of complex form. We consider portable laser scanners as our data acquisition source, as such scanners offer efficient site coverage. Nonetheless, as portable scans are characterized by relatively sparse point clouds and noisy responses, their processing becomes a challenge. While existing research focused on the development of robust estimation methods, their application scope exhibited some limitations in preserving sharp features. Here, we demonstrate how the use of the L_0 norm optimization framework, which features an inherent ability to preserve sharp transitions, with no need to introduce assumptions about the scene structure, can accommodate such a problem. Results show improved performance compared to common normal computation schemes with more reliable and accurate estimations of their form.

1. INTRODUCTION

Surface normals are a fundamental feature used for describing the outline and shape of geometric entities. Therefore, their reliable estimation plays a pivotal role in almost any shape analysis-related application, e.g., feature extraction, geometric and semantic segmentation, denoising, or saliency computation, to name only a few examples (Pauly et al., 2003; Lange and Polthier, 2005; Demarsin et al., 2007; Grilli et al., 2017; Arav and Filin, 2020). Accordingly, the study of reliable methods to compute them has been receiving great attention over the years, specifically while considering the effect of noise and underlying surface form (Sanchez et al., 2020).

In heritage sites, where the shape complexity of architectural details is evident, a reliable and accurate computation of normals becomes even more involved. There, however, considerations of efficient coverage of sites, whose dimensions may be considerable, introduce a trade-off between detail and span (Patrucco et al., 2019; Bronzino et al., 2019). In recent years, the advent of portable laser scanning (PLS) platforms improved accessibility and flexibility of 3-D documentation, allowing to decimate the time on site considerably. However, and in contrast to the more traditional terrestrial laser scans, portable data are sparser and their quality, noise-wise, is low. The noisy nature of PLS data is affirmed by algorithmic failure and poor results in the estimation of geometric primitives reported by related studies (Xia et al., 2020; Wang et al., 2020). In that respect, direct normal estimation from such scans becomes a challenge over complex surface forms and around discontinuous elements (Zhang et al., 2022). Moreover, the ambiguity of the definition of point cloud normals around sharp features remains an ongoing research problem still addressed by research-

ers (Boulch and Marlet, 2012; Huang et al., 2013; Nurunnabi et al., 2015; Zhang et al., 2018; Sanchez et al., 2020).

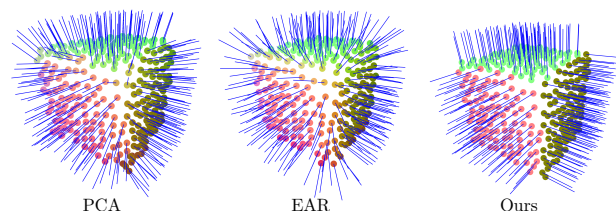


Figure 1. Normal computation of a sparse and noisy point cloud around a corner and an edge linking two faces. Results demonstrate performance of the PCA, edge-aware resampling (EAR), and our L_0 based solution.

Existing research into normal computation has mainly focused on the application of robust estimation methods applied mostly to simple shapes characterized by dense point clouds, and usually required adequate weighting strategy and iterative calculations (Huang et al., 2013). To address the singularity problem, studies either required correct identification of feature points from noisy responses or resorted to heuristics designed for specific cases, i.e., the intersection of two planes (Zhang et al., 2018; Sanchez et al., 2020). As they either require low-level of noise or introduce assumptions about the underlying surfaces, the scope of their application may be limited.

Aiming to address these challenges, we propose in this paper a robust surface normal computation solution based on the L_0 minimization framework. Such a solution addresses the low resolution, noisy responses, and shape complexity. We demonstrate how the singularity around edges can be solved in a simple manner, without the need for the identification of fea-

* Corresponding author

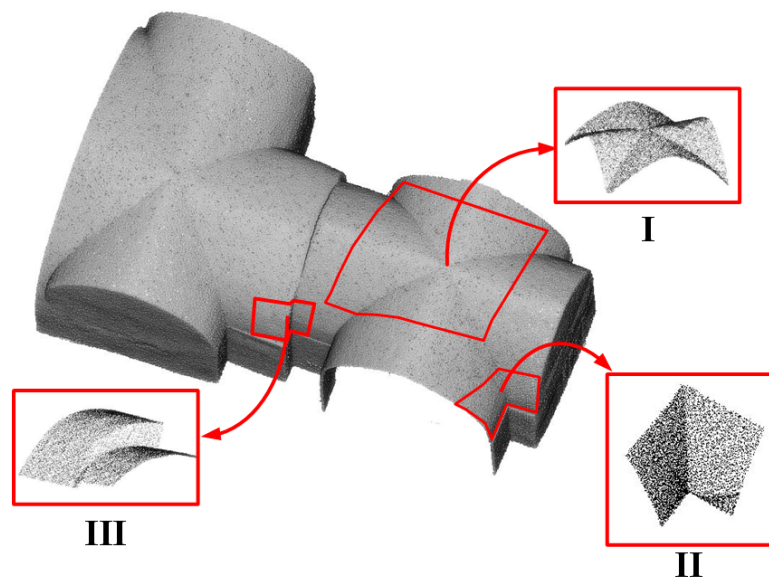


Figure 2. Overview of the selected models on the groin vault

tures from noisy responses. Experiments on complex elements of heritage sites suggest the proposed method outperforms previous studies, visually and quantitatively.

2. RELATED WORK

Early work approached normal estimation by using plane-fitting (Jain and Ho, 1987). Hoppe et al. (1992) proposed to analyze the neighborhood covariance through a principal component analysis (PCA) to deduce the direction. Such estimation is sensitive to noise and is also limited in its assumption of the underlying structure. Later, Sun et al. (2007) proposed to couple surface normal estimation with a point cloud denoising in a two-step strategy that iteratively updates the point normal while smoothing the positions. Similarly, Lipman et al. (2007) and Huang et al. (2009, 2013) presented a locally optimal projection (LOP) operator for points denoising based on the L_1 median and then estimated the surface normals from the consolidated data. Their approaches performed well in the presence of noise and outliers, at the cost of an over-smoothed pointset and the loss of sharp features.

Alternatively, Boulch and Marlet (2012) proposed a direct normal estimation method that utilized a voting strategy inspired by the Hough transformation as a means to extract the actual normals. Such a majority-win approach effectively enhances the discontinuities, yet requires a massive collection of triplets to obtain the discrete probability distribution of possible normals per point. Nurunnabi et al. (2015) proposed a random sampling consensus (RANSAC)-based estimation, by effectively detecting outliers and eliminating their effects. Both methods are robust to outliers yet computationally expensive, hence limited in broader applications.

Zhang et al. (2018) sought a smooth normal field that minimizes a cost function based on weights assigned to neighboring points pairs depending on their normal likeliness. Liu et al. (2020) proposed the computation of normals in transition areas by firstly identifying feature points through orientation discrepancy analysis. The singularity around transitions was solved by iteratively dividing neighbors of features into subgroups through

normal similarity and internal consistency analysis. Such an approach requires the identification of feature points and utilizes normal discrepancy at intersections. Therefore, it is sensitive to noise. Recently, Sanchez et al. (2020) applied M-estimators to estimate normals by an iterative weighted PCA. Their approach sought to identify points on the intersection of surfaces through curvature estimation and initialization of a weighted PCA by providing two initial raw guesses. Zhang et al. (2022) addressed the limitations in multiple plane intersections and proposed to solve the normal ambiguity by employing iterative weighted attributes adjustment. Their approach is based on robust least-squares fitting, and therefore provided high fidelity outcome, but required a careful weighting strategy due to the iterative manner by which it was performed.

Evaluation of the application of most reviewed methods demonstrates that experiments were largely performed on datasets where the actual noise level was limited and the data was relatively dense. Such setups are not prevalent when using common portable laser scanners. The review has also demonstrated that existing approaches address discontinuities in a rather algorithmic manner, usually attempting to handle edges. Being heuristic by nature they are less designed to handle more complex cases.

3. METHODOLOGY

Rather than coupling point cloud denoising and normal estimation, we propose direct attribute optimization using an L_0 minimization by which we obtain a locally smooth and edge-aware normal field. As a starting point, we use the iterative reweighted minimization least-squares (IRLS) method. We compute the eigenvector associated with the smallest eigenvalue of a weighted tensor form. For the set of normalized weights, $\{w_j\}_{j=0, \dots, n}$, associated with the neighbors of a point \mathbf{x}_i , the weighted tensor is defined by Eq. (1):

$$\mathbf{T} = \frac{1}{n} \sum_j^n w_j (\mathbf{x}_j - \bar{\mathbf{x}}) \otimes (\mathbf{x}_j - \bar{\mathbf{x}}) \quad (1)$$

where \otimes is the outer product, \mathbf{x}_j is 3-D neighboring point, $j = 1, \dots, n$, and $\bar{\mathbf{x}}$ is the centroid of the set of points (the mean of neighbor points). Defining $\delta_{j,i} = \mathbf{x}_j - \mathbf{x}_i$, and $r_j = \langle \mathbf{v}_3, \delta_{j,i} \rangle$ the projected distances of $\delta_{j,i}$ on \mathbf{v}_3 , the eigenvector associated with the smallest eigenvalue, we follow Sanchez et al. (2020) strategy to compute:

$$W_j = \left(\frac{\eta}{\eta + r_j^2} \right)^2 \quad (2)$$

and w_j :

$$w_j = \frac{W_j}{\sum_{k=1}^n W_k} \quad (3)$$

where η is firstly initialized as the maximum of squared projection distances and decreases at each iteration to favor smaller inlier residuals. Unlike the plane-fitting-based filtering model, this process is iterative, where we constantly identify outliers and eliminate their effect by adjusting their weights. For speedup, the principal components of \mathbf{T} , given by the eigenvalues and eigenvectors, λ_j and \mathbf{v}_j , such that:

$$\mathbf{T}\mathbf{v}_j = \lambda_j \mathbf{v}_j, \quad j \in \{1, 2, 3\} \quad (4)$$

are computed in a closed-form rather than applying a general decomposition of the roots.

Defining the characteristic polynomial $a\lambda^3 + b\lambda^2 + c\lambda + d = 0$, the eigenvalues are computed as follows:

$$\begin{aligned} \lambda_1 &= \mu + 2\nu \cdot \cos \theta \\ \lambda_2 &= \mu + 2\nu \cdot \cos \theta + 120^\circ \\ \lambda_3 &= 3\mu - \lambda_1 - \lambda_2 \end{aligned} \quad (5)$$

where:

$$\begin{aligned} \mu &= \frac{\text{tr}(\mathbf{T})}{3} \\ \nu &= \sqrt{\frac{\text{tr}((\mu \cdot \mathbf{I} - \mathbf{T})^2)}{6}} \\ \theta &= \frac{1}{3} \cos^{-1} \left(\frac{1}{2} \det(\mathbf{T} - \mu \mathbf{I}) \right) \end{aligned} \quad (6)$$

and \mathbf{I} is a 3×3 identity matrix. The relevant eigenvector \mathbf{v}_3 is the surface normal, and is computed by the cross product of any two rows of $\mathbf{T} - \lambda_3 \mathbf{I}$.

3.1 Normal Field Refinement

By using local point neighborhoods, certain points of other surfaces near sharp edges or corners would inevitably be introduced as neighbors of a studied point. Having refined their original noisy form, we turn to improve their estimation. In contrast to the point-wise normal estimation (Sanchez et al., 2020; Liu et al., 2020) or the robust addition to iterative bilateral normal smoothing (Zhang et al., 2022), we obtain refined orientation field, \mathbf{N} , by minimizing the cost:

$$\underset{\mathbf{N}, |\mathbf{N}_i|=1}{\text{argmin}} \|\hat{\mathbf{N}} - \mathbf{N}\|^2 + \lambda \|D(\mathbf{N})\|_0 \quad (7)$$

where $D(\mathbf{N})_{ik+j} = N_i - N_{M(i,j)}$ and $M(i,j)$ gives the j -th entry in the set of k nearest neighbors of a point i . Therefore, $D(\mathbf{N})$ is a pair-wise normal difference vector. The first term in Eq. (7) is a data fidelity term aimed to ensure that the output

values do not stray too far from the input. The λ value controls how smoothed the output would be. The L_0 norm $\|\cdot\|_0$ directly measures sparsity and allows the sharp transition of normals. Therefore it avoids over-smoothness as with the L_2 norm.

Direct optimization of L_0 norm is nontrivial due to its combinatorial nature. In order to solve this complex optimization problem to create piecewise constant normal field, we introduce a set of auxiliary variables δ and reformulate Eq. (7) as (He and Schaefer, 2013):

$$\underset{\mathbf{N}, |\mathbf{N}_i|=1}{\text{argmin}} \|\hat{\mathbf{N}} - \mathbf{N}\|^2 + \beta \|D(\mathbf{N}) - \delta\|^2 + \lambda \|\delta\|_0 \quad (8)$$

where λ controls the level of variations in the normal field and β is an auxiliary variable. We solve this expression with an alternating optimization. First, we hold $\hat{\mathbf{N}}$ constant and only minimize for δ :

$$\underset{\delta}{\text{argmin}} \beta \|D(\mathbf{N}) - \delta\|^2 + \lambda \|\delta\|_0 \quad (9)$$

In this minimization problem, each entry δ_i can either be 0 or $D(\mathbf{N})$, to either minimize the L_0 norm of δ_i or the L_2 difference with $D(\mathbf{N})$. Therefore, we obtain a simple solution for δ_i as 0 if $\sqrt{\frac{\lambda}{\beta}} > D(\mathbf{N})_i$, otherwise $\delta_i = D(\mathbf{N})_i$. Next, we fix δ and optimize for \mathbf{N} :

$$\underset{\mathbf{N}, |\mathbf{N}_i|=1}{\text{argmin}} \|\hat{\mathbf{N}} - \mathbf{N}\|^2 + \beta \|D(\mathbf{N}) - \delta\|^2 \quad (10)$$

This expression is quadratic in \mathbf{N} , and therefore immediate to minimize. Both of these optimizations alternate until convergence. The L_0 minimization is given in Alg. (1). In this pro-

Algorithm 1: Normal smoothing via L_0 minimizations

Input: Noisy Normals $\hat{\mathbf{N}}$

Output: Refined Normals \mathbf{N}

Initialization: compute $\lambda, N \leftarrow \hat{\mathbf{N}}, \beta \leftarrow 10^{-3}$

```

1 repeat
2   | fix  $\mathbf{N}$ , solve for  $\delta$  in (9)
3   | fix  $\delta$ , solve for  $\mathbf{N}$  in (10)
4   |  $\beta \leftarrow \mu\beta$ 
5 until  $\beta \geq 10^3$ 

```

cedure, μ is the speed at which β is increased. This choice initially set a large threshold by which we determine the value of δ , and gradually reduces the threshold to zero as the optimization continues.

4. RESULTS

We evaluate our normal estimation algorithm on simulated data featuring corners and plane intersections (Figs. 1, 3 & 4) and on architectural elements collected using the GeoSLAM ZEB-REVO portable laser scanner. The latter were collected at the Seraya site (palace in Turkish) in the ancient city of Nazareth, Israel (Figs. 2, & 5). Built around 1730, during the Ottoman era, the Seraya served as the regional ruler's residence, hence its importance.

Throughout our experiments, we set $r = 3$ cm a choice driven by the sensor's point density and noise level. The setting of η

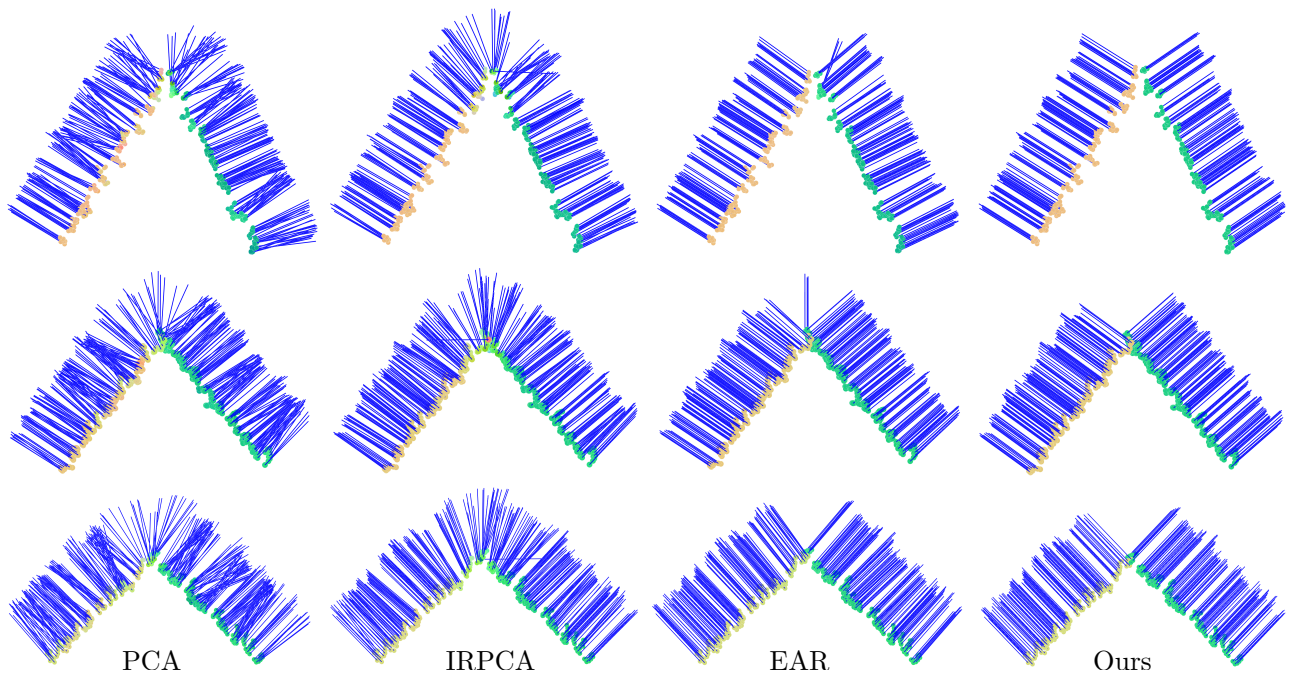


Figure 3. Comparison of our edge-aware normal estimation directly from raw noisy observation comparing to EAR (Huang et al., 2013) and IRPCA (Sanchez et al., 2020), our normal field is piece-wise smooth and also edge-aware.

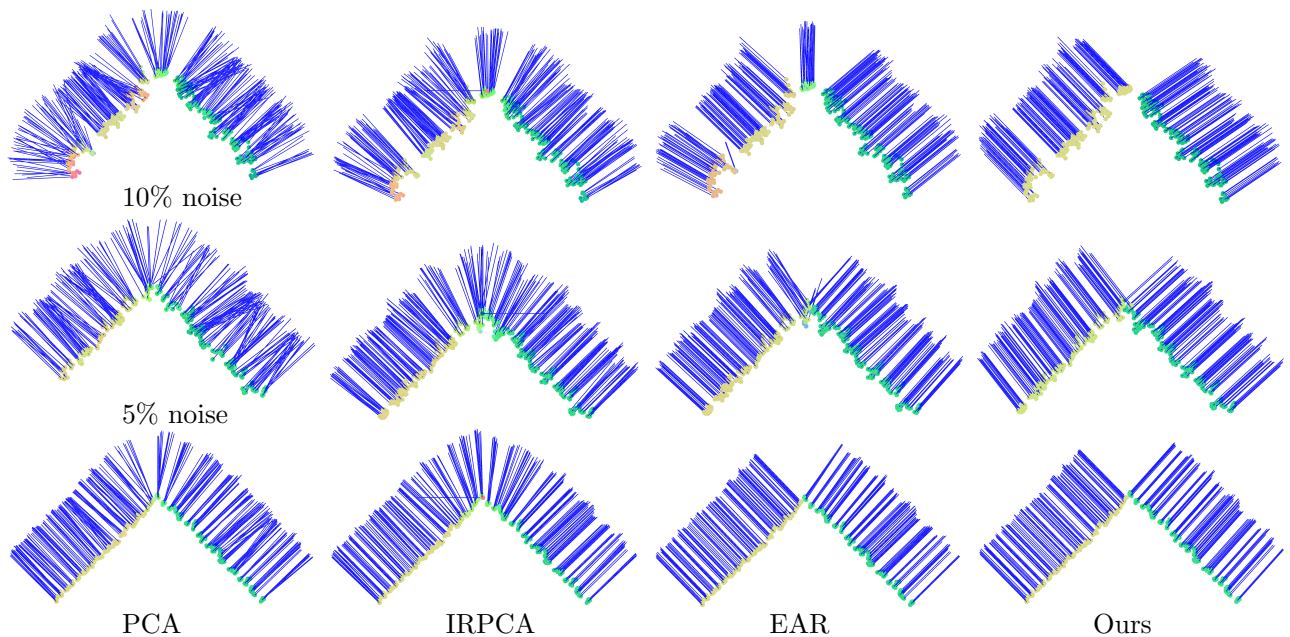


Figure 4. Impacts of noise on the normal estimation comparing to EAR (Huang et al., 2013) and IRPCA (Sanchez et al., 2020), our normal estimation is robust to noise

followed that offered by Sanchez et al. (2020), where the initial value is set to the maximum of squared projected distance. The value of β that weights the variations of normal for the L_0 optimization was set to 0.001 throughout our experiment, and μ , which defines the speed at which β is increased, was set to $\mu = 1.4$. In addition, λ was initialized with 0.004. These settings were defined with consideration of the noisy nature of the initial normal field in mind. Accordingly, we assigned a low weight to the variation at the beginning and gradually increased its weight as the L_0 optimization progressed.

We firstly perform our experiments on synthetic data featuring

varying transition angles and varying noise levels. To demonstrate the improved performance of our model we compare it to the classic edge-aware resampling (EAR) normal estimation (Huang et al., 2013) as well as to the recent iterative re-weighting PCA (IRPCA, Sanchez et al., 2020). In accordance with the portable scanning data characteristics, our point cloud is sparse, making the distinction of the edge-related neighboring points more complicated to define. Of focus in Fig. (3) is the intersection of two planes with sharp and obtuse transition angles. While the PCA, IRPCA, and EAR face some difficulties in distinguishing normals at the intersection point, our method

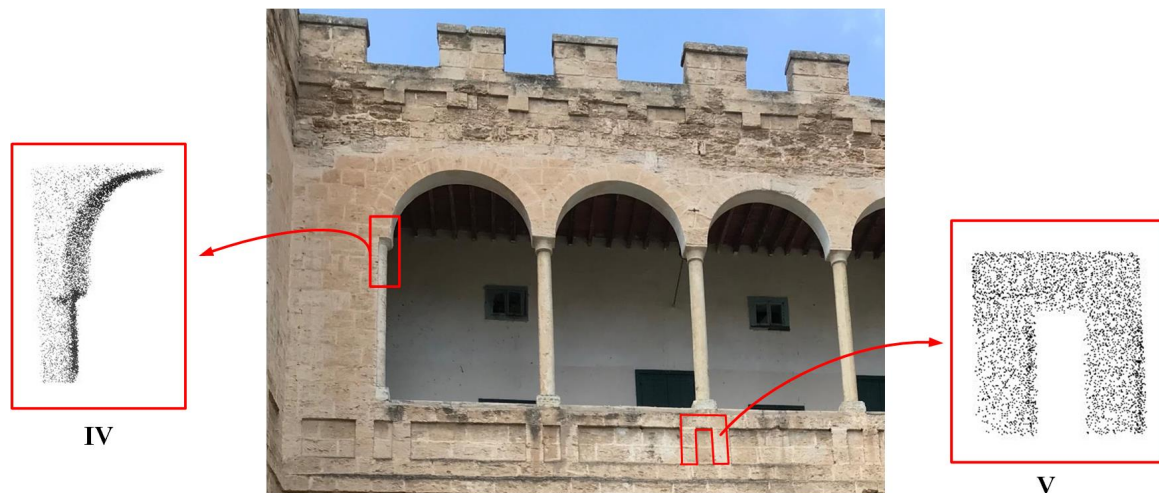


Figure 5. Overview of more models for comparison

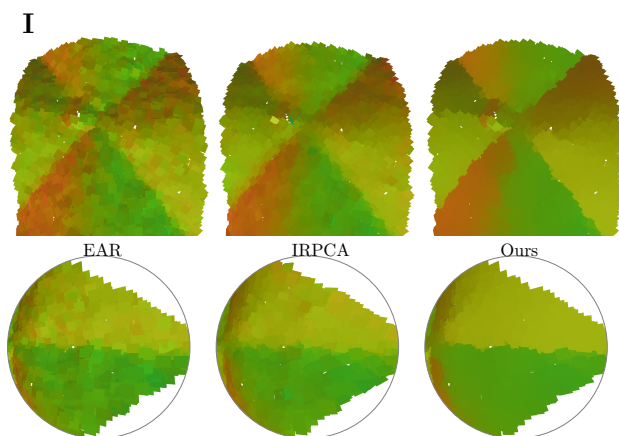


Figure 6. Comparison of our algorithm to EAR (Huang et al., 2013) and IRPCA (Sanchez et al., 2020) at more complex junctions. Points are colored by their normal orientations. Our approach produces a global smooth normal field, while maintaining sharp the transitions without the need to perform denoising.

correctly computes the two groups of normals with a distinct transition. We also demonstrate the robustness of the proposed method when the noise level increases (Fig. 4). Note that when the noise level is low, good results are still obtained when using the EAR. Nonetheless, as the noise level increases, the quality of the normals around the transition area decreases. In contrast, the L_0 based computation remains unaffected. In both experiments (Fig. 3 & 4), our proposed method correctly resolved the ambiguity at the sharp transition and computed high fidelity normals regardless of the noise level and in the presence of sparse data.

For the real-world experiments, we select a set of representative elements from the Seraya site. The first set is from two adjacent chambers each covered by a groin vault, and ones from the facade of the inner courtyard (Fig. 2). Fig. (6) shows the normal computation results for the groin vault. The direct application of the EAR uses the raw PCA computation as its base, showing that the noise level of the raw data affects the quality of the normal estimation. Better results are obtained when using the robust PCA approach, but noise can still be observed.

The application of our approach produces smoother results as well as sharper edge preservation. For a close-up inspection of the normal distribution around profiles in this dataset (Fig. 2) we evaluate the normals around a corner of one of the chambers, where two flanks of the vault intersect, and at the transition between the two chambers (II & III in Fig. 2, respectively). Results in Fig. (7) demonstrate how our approach performs well at these rapid transition areas between two and three surfaces (again despite the high noise level and low point density), and yields accurate normals compared to the other strategies. Similar performance can be observed for features on the facade of the inner courtyard at the site (Fig. 5) where variations between object and background are even more subtle. Around the capital of a supporting column (IV in Fig. 5), where both capital and column are non-planar entities, our normals computation yields more consistent results compared to the counterpart methods (Fig. 8). Consistency in the normal computation is also observed around projecting and receding wall patterns that form a set of parallel planar surfaces (V in Fig. 5), where again the lower resolution affects the computation of other methods compared to ours (Fig. 9). Finally, we demonstrate the application of our method on a pointed arch (Fig. 10), again demonstrating that despite the low density and noise, high quality estimated normals were obtained.

For quantitative analysis we measure the closeness of our estimated normal to ground truth information, using the discrepancy of normals on the selected element for evaluation (V in Fig. 5). We perform the analysis on the brickwork wall pattern to demonstrate the improvement of attribute estimation by our model. For such a form (Fig. 9), we expect an agreement of normals in local regions, with only minor variations. To quantify this, for each point x_i , we analyzed the angular similarity to the normal of each point in its k -neighborhood ($k = 100$) and analyzed the distribution of overall normal similarity. As demonstrated in Fig. (11), our model has the lowest variation of normals on the plane model.

5. CONCLUSIONS

Recognizing that surface normals play a pivotal role in most shape analysis applications, this paper studies robust means for their estimation. As input data it considered portable laser scans that can offer an efficient site coverage. Using such input

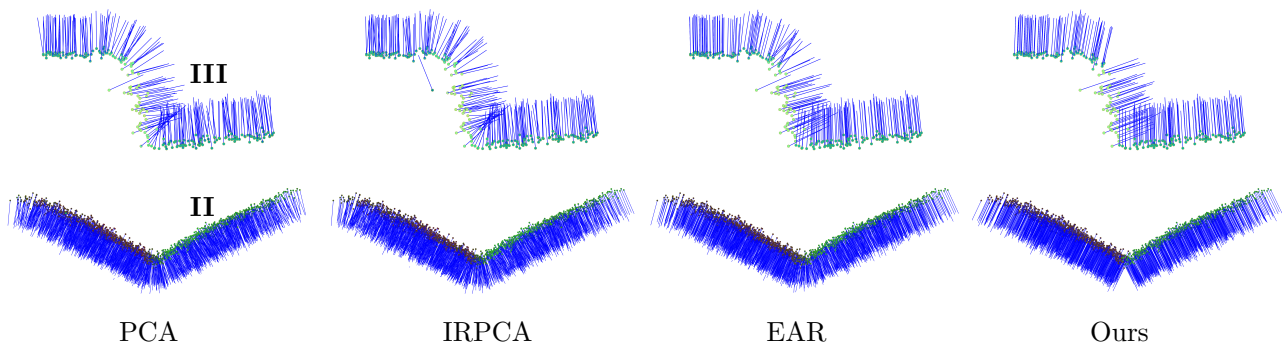


Figure 7. Comparison of our edge-aware normal estimation directly from raw noisy observation comparing to EAR (Huang et al., 2013) and IRPCA (Sanchez et al., 2020), our normal field is piece-wise smooth and also edge-aware.

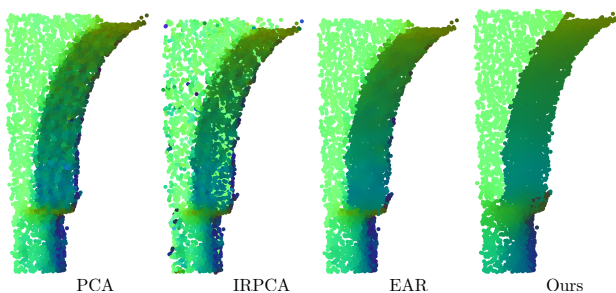


Figure 8. Normal estimation outcome of the supporting pillar (Model IV)

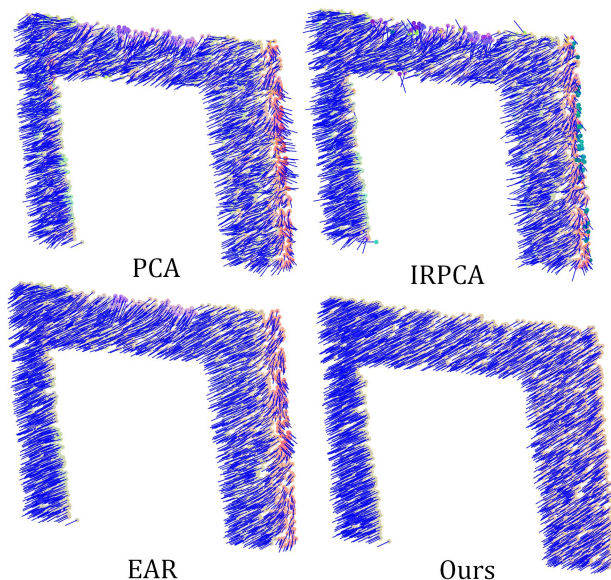


Figure 9. Normal estimation outcome of the parallel planes (Model V)

data, consideration of sparse point clouds and noisy response were processing challenge to tackle. The paper has demonstrated how prevailing strategies have faced difficulty in handling sparsity and noisy responses, mostly due to the algorithmic considerations they introduced. To address that the paper proposed the introduction of the L_0 norm optimization framework, which features an inherent ability to preserve sharp transitions with no need to introduce assumptions about the scene structure. Through a set of experiments on both simulated and real-

world data it has demonstrated that such an approach yields better performance in the computation of normals around complex transitional regions, and despite the low data quality.

6. ACKNOWLEDGMENTS

The authors would thank the Nazareth old city committee and the Nazareth municipality for their support.

REFERENCES

- Arav, R., Filin, S., 2020. Saliency of Subtle Entities Within 3-D Point Clouds. *ISPRS Annals of the Photogrammetry, Remote Sensing and Spatial Information Sciences*, 2, 179–186.
- Boulch, A., Marlet, R., 2012. Fast and robust normal estimation for point clouds with sharp features. *Computer graphics forum*, 31number 5, Wiley Online Library, 1765–1774.
- Bronzino, G., Grasso, N., Matrone, F., Osello, A., Piras, M., 2019. Laser-visual-inertial odometry based solution for 3D heritage modeling: the sanctuary of the blessed virgin of trompone. *International Archives of the Photogrammetry, Remote Sensing & Spatial Information Sciences*.
- Demarsin, K., Vanderstraeten, D., Volodine, T., Roose, D., 2007. Detection of closed sharp edges in point clouds using normal estimation and graph theory. *Computer-Aided Design*, 39(4), 276–283.
- Grilli, E., Menna, F., Remondino, F., 2017. A review of point clouds segmentation and classification algorithms. *The International Archives of Photogrammetry, Remote Sensing and Spatial Information Sciences*, 42, 339.
- He, L., Schaefer, S., 2013. Mesh denoising via L_0 minimization. *ACM Transactions on Graphics (TOG)*, 32(4), 1–8.
- Hoppe, H., DeRose, T., Duchamp, T., McDonald, J., Stuetzle, W., 1992. Surface reconstruction from unorganized points. *Proceedings of the 19th annual conference on computer graphics and interactive techniques*, 71–78.
- Huang, H., Li, D., Zhang, H., Ascher, U., Cohen-Or, D., 2009. Consolidation of unorganized point clouds for surface reconstruction. *ACM transactions on graphics (TOG)*, 28(5), 1–7.
- Huang, H., Wu, S., Gong, M., Cohen-Or, D., Ascher, U., Zhang, H., 2013. Edge-aware point set resampling. *ACM transactions on graphics (TOG)*, 32(1), 1–12.

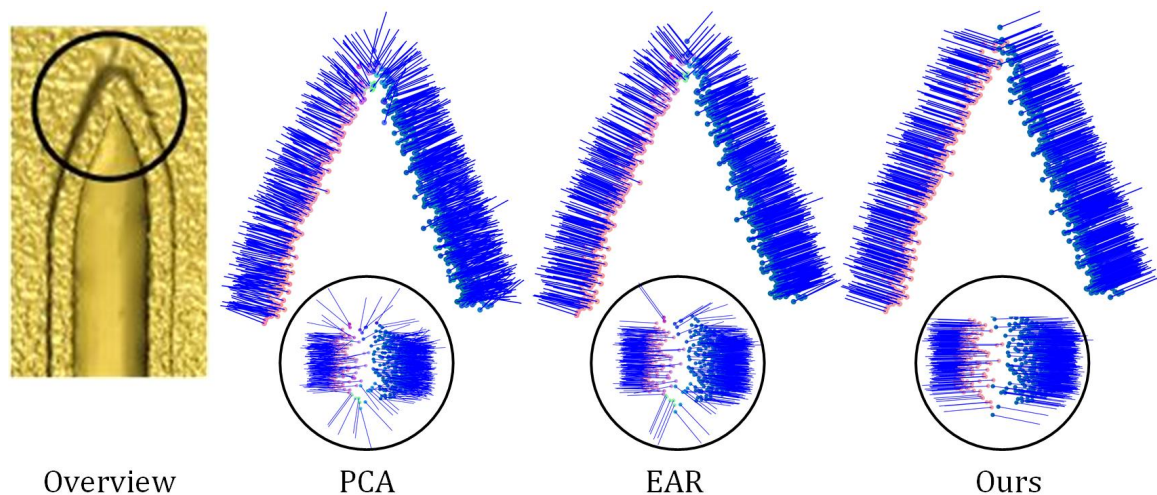


Figure 10. Comparison of our edge-aware normal estimation directly from raw noisy observation comparing to EAR and IRPCA, our normal field is piece-wise smooth and also edge-aware.

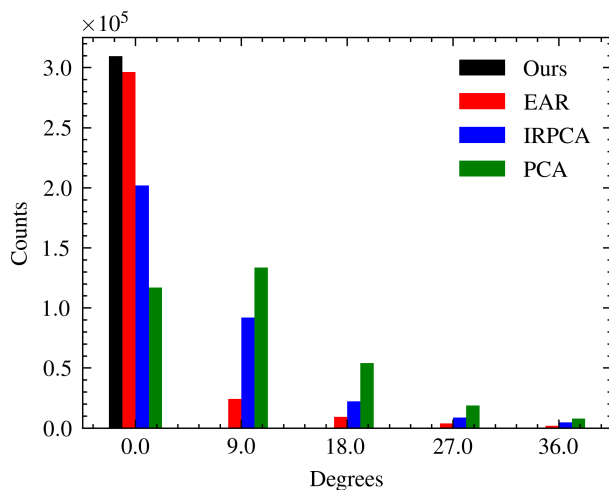


Figure 11. Normal estimation outcome of the supporting pillar (Model V)

Jain, A., Ho, R., 1987. man, Segmentation and classi” cation of range images. *IEEE Trans. Pattern Anal. Mach. Intell.*, 9(9).

Lange, C., Polthier, K., 2005. Anisotropic smoothing of point sets. *Computer Aided Geometric Design*, 22(7), 680–692.

Lipman, Y., Cohen-Or, D., Levin, D., Tal-Ezer, H., 2007. Parameterization-free projection for geometry reconstruction. *ACM Transactions on Graphics (TOG)*, 26(3), 22–es.

Liu, Z., Xiao, X., Zhong, S., Wang, W., Li, Y., Zhang, L., Xie, Z., 2020. A feature-preserving framework for point cloud denoising. *Computer-Aided Design*, 127, 102857.

Nurunnabi, A., West, G., Belton, D., 2015. Outlier detection and robust normal-curvature estimation in mobile laser scanning 3D point cloud data. *Pattern Recognition*, 48(4), 1404–1419.

Patrucco, G., Rinaudo, F., Spreafico, A., 2019. Multi-source approaches for complex architecture documentation: the” Palazzo Ducale” in Gubbio (Perugia, Italy). *International Archives of*

the Photogrammetry, Remote Sensing & Spatial Information Sciences.

Pauly, M., Keiser, R., Gross, M., 2003. Multi-scale feature extraction on point-sampled surfaces. *Computer graphics forum*, 22number 3, Wiley Online Library, 281–289.

Sanchez, J., Denis, F., Coeurjolly, D., Dupont, F., Trassoudaine, L., Checchin, P., 2020. Robust normal vector estimation in 3D point clouds through iterative principal component analysis. *IS-PRS Journal of Photogrammetry and Remote Sensing*, 163, 18–35.

Sun, X., Rosin, P. L., Martin, R., Langbein, F., 2007. Fast and effective feature-preserving mesh denoising. *IEEE transactions on visualization and computer graphics*, 13(5), 925–938.

Wang, C., Wen, C., Dai, Y., Yu, S., Liu, M., 2020. Urban 3D modeling with mobile laser scanning: a review. *Virtual Reality & Intelligent Hardware*, 2(3), 175–212.

Xia, S., Chen, D., Wang, R., Li, J., Zhang, X., 2020. Geometric primitives in LiDAR point clouds: A review. *IEEE Journal of Selected Topics in Applied Earth Observations and Remote Sensing*, 13, 685–707.

Zhang, J., Cao, J., Liu, X., Chen, H., Li, B., Liu, L., 2018. Multi-normal estimation via pair consistency voting. *IEEE transactions on visualization and computer graphics*, 25(4), 1693–1706.

Zhang, T., Abu-Hani, J., Filin, S., 2022. Shape preserving noise attenuation model for 3-d-modeling of heritage sites by portable laser scans. *The International Archives of Photogrammetry, Remote Sensing and Spatial Information Sciences*, 46, 551–556.